

Effect of Thermal Treatment on Magnesite Impurity Removal Using Dry High-Intensity Magnetic Separation

Mohammed S. Alhaddad and Hussin A. M. Ahmed

*King Abdulaziz University, Jeddah, Faculty of Engineering, Mining Engineering Department
malawialhaddad@stu.kau.edu.sa*

Abstract: This study investigates the extraction of impurities from a low-grade Saudi magnesite ore with the following composition: 37.68% MgO, 7.24% CaO, 3.10% SiO₂, 1.91% Fe₂O₃, 0.58% Al₂O₃, and 48.65% LOI. Additionally, it examines the calcination process of magnesite and the subsequent removal of impurities. Dry high-intensity magnetic separation was utilized for the magnesite both before and after calcination. Various parameters, including feed size, feed rate, magnetic field strength, and roll speed, were assessed using an Outotec-induced roll magnetic separator (model MIH 13 111-5). The results demonstrate that impurity removal and recovery are more efficient after calcination than before. The final product is anticipated to be a suitable raw material for producing dead-burned magnesia, which is utilized in the refractory industry.

Keywords: magnesite, refractory, impurities, calcination, DHIMS.

1. Introduction

Magnesite ore, a deposit of magnesium carbonate, predominantly contains MgO, CO₂, and varying levels of impurities, including iron. Magnesite is a significant source of magnesia (MgO), a crucial refractory material [1,2]. Magnesia is commonly employed as a refractory oxide in furnaces, kilns, and other high-temperature devices due to its high melting point, thermal stability, low thermal expansivity, and excellent resistance to slag [3]. Magnesia makes for roughly 90% of the overall usage for the manufacturing of refractory materials [4,5].

Magnesite deposits typically contain heterogeneous impurities, such as iron, which react with magnesia to form compounds and phases with lower melting points. It is crucial to consider the presence of iron impurities in the magnesite sample as they can significantly affect the quality of the final product. However, a small percentage of iron acts as a binding agent that will help close the porosity, which is beneficial for refractory. Magnesium oxide with ferric oxide closes the pores by cementing them together. This leads to less porosity, which means less reactivity [6,7]. This will be an issue when producing CCM powder because achieving the ideal density will be challenging due to the act of iron impurities as binding agents. Furthermore,

these impurities can affect the compacting conditions of ceramic bodies, resulting in suboptimal density, particularly in processes involving low-density refractories [8].

Iron impurities can be removed or reduced before or after the calcination process. Magnetic susceptibility highly depends on the heating temperature level and particle size. Moreover, the weak magnetic phases tend to increase with temperature, while the strong magnetic phases decrease with increasing. Therefore, it is important to study their behaviour during heat treatment to determine the optimal temperature level [9]. Removing iron impurities in most contributes to reducing other impurities, such as dolomite and silica [10,11].

Studies have shown that the magnetic properties of materials undergo a phase transition during thermal treatment. For instance, a paramagnetic material can transform into a ferromagnetic material and vice versa as the temperature increases. In a previous experimental study, it was found that subjecting magnetite to heat treatment at 600°C for 1-2 hours resulted in the development of hematite phases. Furthermore, heat treatment at 700-800°C for 1-3 hours exclusively led to the formation of the hematite phase [12]. These observations align with the theory that magnetic materials lose or weaken their magnetic properties as temperature rises. Consequently, employing elementary magnetic separation before calcination can help reduce iron impurities, particularly in magnetite. For the paramagnetic transformation into a ferromagnetic mineral phase, heating hematite to 250°C significantly increases its magnetic susceptibility [13,14]. In a separate study, a goethite sample with a particle size of -2 mm was sourced from an iron ore reject stream in the Pilbara region of Western Australia. Roasting the samples at 700°C and 750°C substantially enhanced magnetic separation recovery by transforming

goethite and hematite into magnetite. It's worth noting that the optimal temperature for the goethite to hematite transformation is 450°C in air and (5% CO₂) gas mixtures. Similarly, the preferred temperature range for the transformation of hematite to magnetite is between 650°C and 700°C [15,16].

When applying these temperature levels, it is also a must to consider the magnesite calcination or decomposition temperature level to avoid impacting carbonate impurities. The process of magnesite calcination involves the thermal breakdown of magnesite into magnesia and carbon dioxide. The decomposition of magnesite takes place within a range of temperatures of 300 to 700 [17-22]. The data reveals a distinct sharp peak corresponding to magnesite decomposition and a broad endothermic peak at lower temperatures, usually occurring in the 250–450°C range, attributed to the evaporation of moisture and the elimination of volatile materials [18,21].

Numerous studies have been conducted in magnesite decomposition. In a previous study, a Padamarang magnesite ore in Indonesia exhibited the lowest decarbonization temperature. The formation of magnesite from thin and flat hexagonal sheets suggested the presence of MgO, while the needle-shaped morphology indicated the presence of CaO impurities. The EDX analysis revealed that magnesite contained 30.69% Mg, 15.37% C, and 53.39% O. The calcination experiments involving 2 g of the sample were carried out in a tube furnace at temperatures ranging from 150 to 900°C for 30 minutes. The decomposition occurred within a temperature range of 300 to 400°C, likely close to 400°C, consistent with a previous study by Weast in 1978. XRD analysis showed the disappearance of most MgCO₃ peaks above 300°C during calcination, accompanied by the emergence of MgO peaks, which increased with higher calcination temperatures [17]. Another

study was done on various combinations by mass of MgCO_3 mixed with epoxy resin. The results show a 60% mass reduction for MgCO_3 when the maximum temperature is set to 1000 °C to form MgO . The decomposition begins at 500 °C and is completed at around 550 °C in a Helium gas environment [21]. Another study has indicated that a CO_2 atmosphere raises the ultimate decomposition temperature to approximately 598°C. [22]. In another investigation on Savinski magnesites in Russia known for their large crystalline rocks featuring a radial-radiant "stellar" texture. Impurity rocks contain 0.85% dolomite, 1.60% quartz, and 0.80% pyrite. Fine-grained magnesite rock samples were treated at temperatures ranging from 400 to 1000 °C, with an hour-long exposure at the end temperature. Thermo-analysis of the magnesite sample revealed decarbonization and the formation of magnesium oxide occurring at 606.5 °C. Another type of magnesite from Khalilovski, Russia, exhibits an amorphous form with a crystalline structure only observable under a microscope. The Khalilovski deposit is characterized by serpentine magnesites with a chemical composition of 48.22% MgO , 6.16% SiO_2 , and 2.33% CaO . Heat treatment of the amorphous magnesite at the same conditions led to decarbonization at 579.2 °C, while larger particles underwent decarbonization at 702.3 °C [19]. Also, another test has been done on a magnesite sample obtained from the Afzal Abad mine in Iran, with a chemical composition of 41.85% MgO , 6.16% SiO_2 , and 2.06% CaO , along with the phase of impurities such as dolomite, quartz, kaolinite, olivine, and illite. The TG test used a 50 mg sample in an alumina cell in an air atmosphere, heating at 10 K/min up to 1400 °C. The TG results exhibited a sharp weight loss at 600–650 °C [18]. Finally, A magnesite sample sourced from Uralasbest, Asbest, and the Sverdlovsk region, containing 44.65% MgO , 2.05% SiO_2 , and 1.14% CaO , was subjected to calcination. The decomposition process

began at 578.2°C, with the peak thermal effect of decarbonization occurring at 680.6°C. The magnesite exhibited a weight loss of 51.20% commencing at 642°C [23]. Considering the behavior of magnesite and iron impurities before applying magnetic separation will lead to effective separation, especially for calcined magnesite.

Many researchers studied the magnetic separation methods in magnesite and calcined magnesite. For example, in a study on calcined magnesite from the Mútnik deposit in Slovakia, the magnesite recovery reached 95.81% using DHIMS [24]. In another study, magnesite tailings from KUMAŞ in Turkey containing 77.69% MgCO_3 and 3.14% Fe_2O_3 were subjected to high-gradient magnetic separation twice at 1.8T, resulting in an increase in magnesite content to 91.03% and a reduction in iron content to 0.32% [25]. Furthermore, a study on a representative magnesite-dolomite sample from Wadi El-Barramiya, Egypt, with 33.92% MgO , 7.18% Fe_2O_3 , and CaO , showed that dry magnetic separation effectively separated magnesite stained with hematite and magnetite from dolomite. This resulted in a magnesite concentrate product with 1.12% CaO and 46.02% recovery and a middling fraction containing 44.63% magnesite and 10.95% dolomite [26]. A separate investigation was conducted on calcined magnesite containing 87% MgO , 5% CaO , 4.5% SiO_2 , and 2.6% Fe_2O_3 . The application of dry magnetic separation yielded a product with 92.5% MgO , 2.5% CaO , 2.10% SiO_2 , and 1.54% Fe_2O_3 [11]. Furthermore, dry magnetic separation was applied to calcined magnesite sourced from Eskisehir, Turkey, with 87.99% MgO , 3.2% SiO_2 , and 0.9% Fe_2O_3 , resulting in an increase in MgO by 1.58%, a reduction in SiO_2 by 2.24%, and a reduction in Fe_2O_3 by 0.47% [27]. Lastly, high-gradient magnetic separation (HGMS) and superconducting magnetic separators were utilized on decarbonized magnesite with a particle size of -0.35 mm, yielding a product containing 0.16% SiO_2 and 0.31%

CaO [28]. However, the paper aims to investigate DHIMS before and after magnesite calcination and study Saudi low-grade magnesite ore's calcination or decomposition and impurities.

2. Material and methods

2.1 Materials and sample preparation

The magnesite ore used in the experiment was obtained from the Al Ghazala mine, Hail, Saudi Arabia. Initially, the ore was crushed to -2 mm using a Jaw crusher. The sample was then prepared using the coning and quartering method, followed by the riffle distributor. Subsequently, a portion of the samples were subjected to calcination. The experimental procedure involved exposing the magnesite to temperatures ranging from 500 to 800°C for 0.5, 1, and 1.5 hours soaking at each temperature. A CHM-60H laboratory furnace from Jimbomb Enterprise Co., Ltd., Taiwan, was employed for the calcination. Individual 300 g portions of the magnesite sample were placed in separate cups and then put into the furnace at room temperature (25°C). The heating cycle proceeded at 20°C per minute until the desired temperature was reached. Subsequently, the samples were left to soak for the predetermined period during the cooling cycle, which was uncontrolled. Upon removal from the furnace at 100°C, the samples were placed in a desiccator to prevent moisture absorption and weighed. A ball mill was used for additional size reduction for the subsequent test conditions on magnesite ore or calcined magnesite.

2.2 Methods

2.2.1 Magnesite characterization

The chemical composition was determined using X-ray fluorescence (XRF). Additionally, the iron phases were identified through X-ray diffraction (XRD). These analyses were conducted on magnesite ore, calcined magnesite, and DHIMS

concentration results before and after calcination.

2.2.2 Dry high-intensity magnetic separation

The magnesite ore and calcined magnesite underwent dry high-intensity magnetic separation using the Outotec-induced roll MIH (13) 111-5 model. **Table 1** details the parameters tested for the magnesite ore under initial conditions, with a feed rate of 0.6 kg/min, a roll speed of 40 rpm, and a magnetic field of 12K gauss. The DHIMS test for the calcined magnesite was conducted based on the optimal findings from the DHIMS test of magnesite ore. Finally, the results of DHIMS before and after calcination were compared.

Table 1: DHIMS experiments conditions on magnesite ore

Parameter	Conditions
Feed size (mm) at P ₈₀	-0.63, -0.425, -0.212, -0.1
Feed rate (kg/min)	0.3, 0.9, 1.2
Field intensity (1000*gausses)	8, 10, 14
Roll speed (rpm)	30, 50, 60

3. Result and discussion

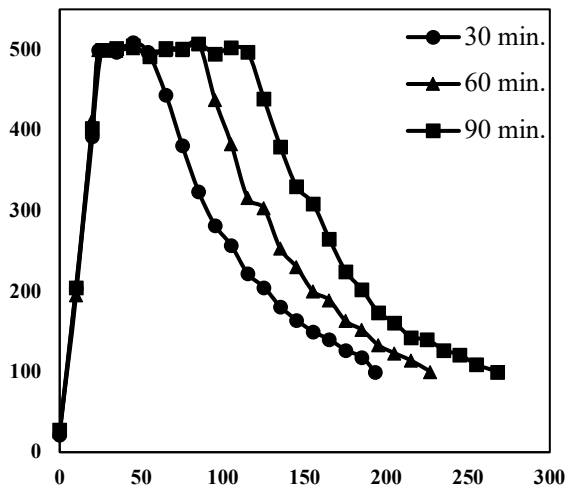
3.1 Magnesite calcination

The graph in (**Figure 1**) shows the furnace's heating conditions during soaking periods lasting 0.5, 1, and 1.5 hr of soaking at peak temperatures of 500°C, 600°C, 700°C, and 800°C. The heating rate is 20°C per minute, and the soaking procedures were consistent across all experiments. It is noted that as the temperature increases, the cooling process requires more time.

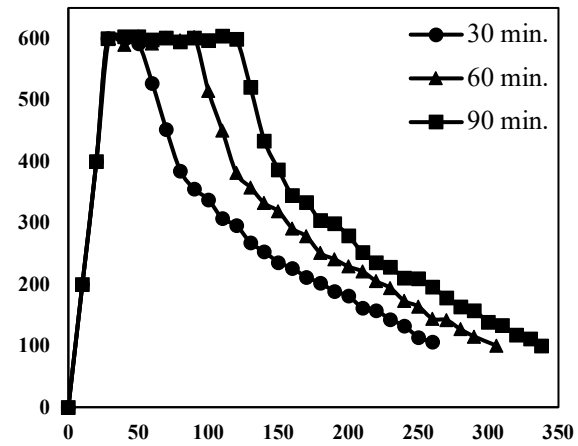
The data in (**Figure 2**) illustrates the weight loss percentages of magnesite samples at different temperatures and heating durations. The results emphasize the substantial influence of temperature and heating duration on the thermal behavior of magnesite. The general impact of heating

time at 0.5 and 1 hour is more pronounced than that at 1 and 1.5 hours, particularly at temperatures of 700°C and 800°C. However, the difference in impact at 1 hour

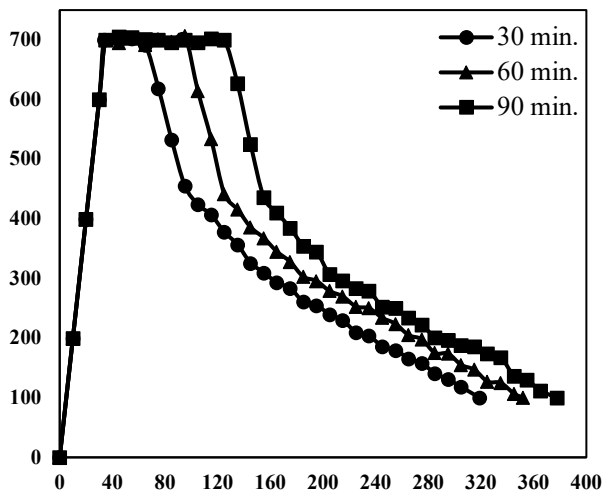
and 1.5 hours becomes negligible, especially at 800°C.



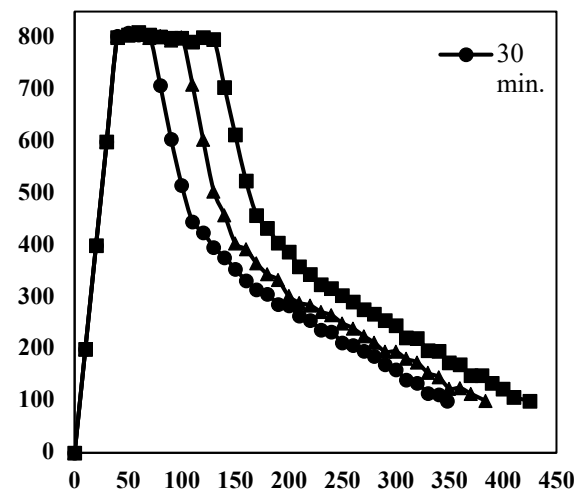
X-axis (time, Min.); Y-axis (temperature, 500°C)



X-axis (time, Min.); Y-axis (temperature, 600°C)



X-axis (time, Min.); Y-axis (temperature, 700°C)



X-axis (time, Min.); Y-axis (temperature, 800°C)

Figure 1: Heating, soaking, and cooling process during partial calcination.

For temperature, the general trend is at lower temperatures, and weight reduction is low due to moisture removal and organic material combustion. At higher temperatures, the weight decrease is high, indicating material decomposition [18,21]. Negligible weight loss is observed at 500°C, even with longer exposure times, resulting in only a 1% reduction after 1.5 hours of heat exposure. At 600°C, the behavior of the magnesite samples becomes more noticeable, particularly at exposure times of 1 and 1.5 hours, with a 7.12%

weight reduction. However, this impact is similar to what was observed in the LOI test, which showed significant decomposition that begins around 600°C. Between 600 and 700°C, the decomposition peak is reached, which matches the high mass reduction rate, with weight loss increasing to 19.52% at 1.5hr. The weight loss stabilizes somewhat at 800°C, indicating that the thermal decomposition of magnesite is nearly complete, resulting in a 21.03% weight reduction.

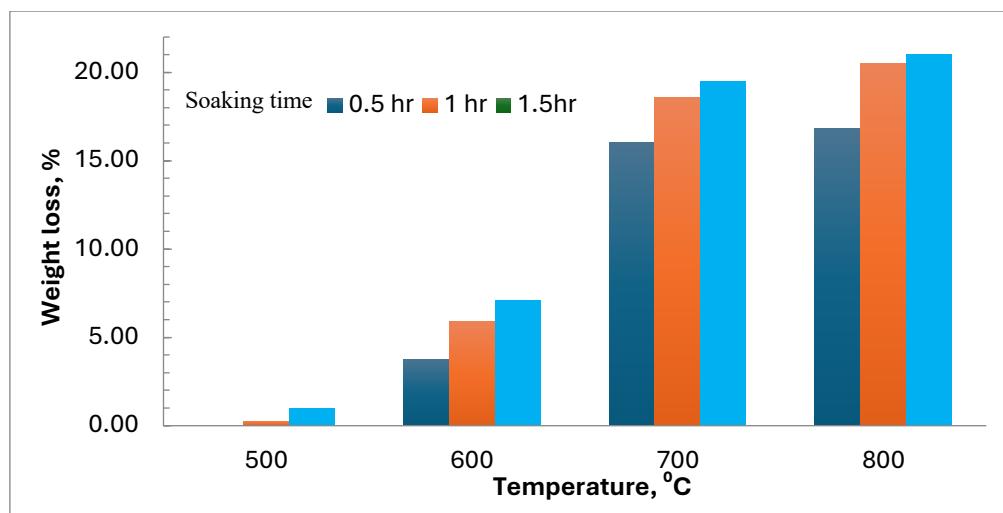


Figure 2: Effect of temperature and heating duration on weight loss of magnesite samples.

3.2 Magnesite characterization

3.2.1 Magnesite ore

The XRD results in (Figure 3) of the magnesite sample show the phase of the ore and all the gangue minerals. The phases within the sample are magnesite, dolomite, quartz, and hematite. The magnesite mineral phase (MgCO_3) was the dominant one and was responsible for most of the four intense peaks, with the highest being 32.69° , 43.01° , 53.89° , and 35.95° . The lower intense peaks of magnesite were observed at 38.87° , 46.99° , 61.42° , 62.43° , 66.42° , 68.36° , 69.33° , 70.37° , 76° . The sample is relatively abundant with dolomite mineral phase ($\text{CaMg}(\text{CO}_3)_2$) with less intense peaks at 35.31° , 50.63° , 51.26° , and 59.88° . The minor phases of the quartz mineral phase (SiO_2) have peaks at 20.91° and 26.69° , and the hematite mineral phase (Fe_2O_3) has peaks at 24.17° and 56.19° .

The XRF analysis of the magnesite sample indicates a high concentration of magnesite

along with impurity minerals. The sample consists of 37.68% MgO , 7.24% CaO , 3.10% SiO_2 , 1.91% Fe_2O_3 , 0.58% Al_2O_3 , and 48.65% LOI. The chemical composition determined by XRF is consistent with phases identified through XRD analysis, except for the alumina content, which XRD does not detect. The significant CaO content suggests contamination from calcium-bearing minerals, particularly dolomite, associated with magnesite deposits, as confirmed by XRD. The presence of SiO_2 indicates the existence of siliceous materials, primarily quartz, while Fe_2O_3 suggests iron contamination from hematite minerals. The minor presence of Al_2O_3 indicates alumina-bearing impurities. The analysis revealed that the impurity content exceeded the required limit. Although the percentage of alumina oxide presence is acceptable, dolomite is the primary gangue mineral.

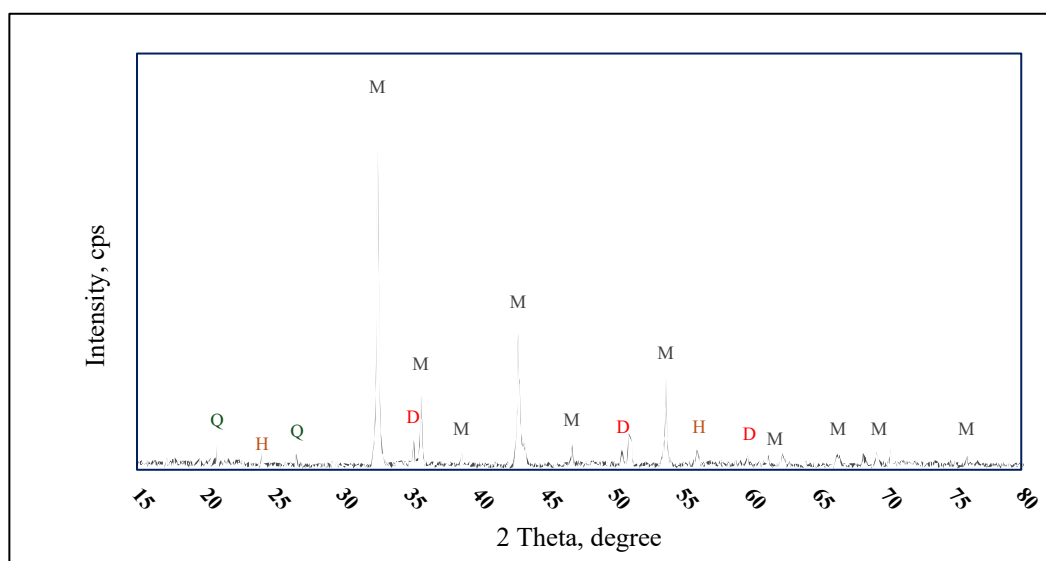


Figure 3: X-ray diffraction for Saudi-low grade magnesite ore

3.2.2 Calcined magnesite

XRD analysis in **(Figure 4)** demonstrates the phase variations observed in magnesite samples at different temperatures (500°C, 600°C, 700°C, and 800°C). At 500°C, mineral phases have no impact, which aligns with the negligible weight reduction at this temperature. Upon reaching 600°C, a new intense peak at 43.01° and a smaller peak at 37.06° were observed for the periclase phase (MgO), while the peaks corresponding to the magnesite mineral phase at 35.95°, 43.01°, and 46.99° disappeared. The dolomite, quartz, and hematite phases remained unchanged. Advancing to 700°C resulted in the disappearance of all magnesite phases, with new peaks corresponding to the periclase phase at 62.26°, 74.75°, and 78.63°. Simultaneously, the hematite phases vanished, and peaks associated with the magnetite phase (Fe_3O_4) emerged at 18.38° and 57.16°. The quartz phase remained unaffected by the increasing temperature. Finally, at 800°C, the peaks of dolomite disappeared, and peaks characteristic of calcite (CaCO_3) were identified at 29.48° and 47.51°. The decomposition of dolomite occurred between 700 to 800°C, which is a relatively low decomposition temperature

but consistent with previous studies [21,29]. However, it is worth noting that the decomposition could also be attributed to rapid heating, and it should be below 10°C/min, as found by [23]. Notably, the quartz phase exhibited no impact even at this elevated temperature. In **(Figure 5)**, the variation in MgO content in the sample is depicted at different temperatures (500°C, 600°C, 700°C, and 800°C) over time intervals of 0.5, 1.0, and 1.5 hours. At 500°C, the MgO content remains relatively stable, around 37.67% to 37.68% across the time intervals. This indicates that the temperature is insufficient to impact the magnesite mineral, consistent with XRD and LOI results. At 600°C, there is an initial increase in MgO content (3.65-6.96%) compared to 500°C, and the impact of exposure time at this temperature level was 3.33%. This suggests the onset of magnesite decomposition, but at the same time, was a relatively slow rate even with extended heat exposure, reaching up to 44.65%. Additionally, not all magnesite decomposes at this temperature level, as confirmed by the XRD results showing magnesite and periclase peaks, and like the previous findings [22]. The MgO content shows a significant increase at 700°C

(13.75-14.91%) compared to a temperature level of 600°C, with a 4.49% impact of exposure time. This significant thermal decomposition aligns with the XRD result

of showing only periclase peaks, corresponding to increases in the concentrations of MgO content by up to 59.56%.

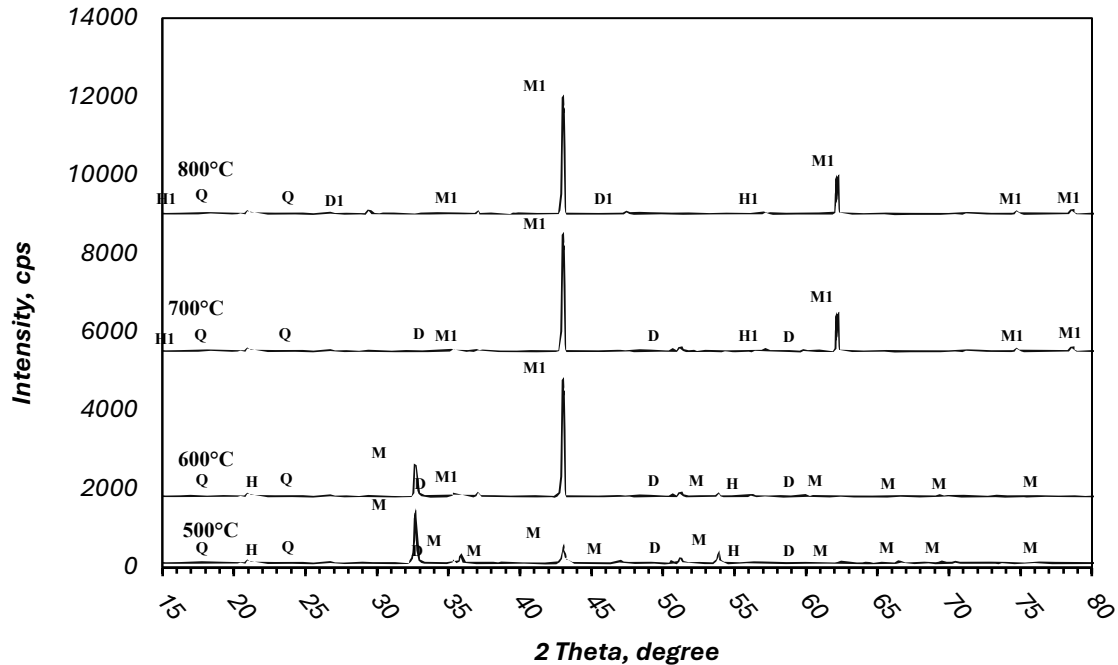


Figure 4: X-ray diffraction patterns of magnesite samples heated at different temperatures (M: magnesite, M1: periclase (MgO), D: dolomite, D1: calcite, H: hematite, H1: magnetite Q: quartz).

These findings are consistent with previous research on magnesite decomposition within similar ranges of temperature levels [18,19,22]. Finally, at 800°C, the MgO content exhibits a slight increase (6.52%) compared to the previous temperature level, stabilizing at 64.22% after 1.5 hours of partial calcination. The impact of exposure time at 800°C temperatures was lower, 2.63%, indicating that the magnesite decomposition ends.

The data presented in **(Figure 6)** illustrates the changes in CaO content over time intervals of 0.5, 1.0, and 1.5 hours at varying temperatures (500°C, 600°C, 700°C, and 800°C). At 500°C and 600°C, the CaO content remains relatively stable,

ranging between 7.23% and 7.25% across these temperature and time intervals. However, a slight increase is observed at 700°C, where the CaO content rises more noticeably, reaching around 7.32% at 1.5 hours. The absence of signs of dolomite decomposition in the XRD results suggests that this slight increase might be due to mass reduction in the sample because of magnesite decomposition. At 800°C, there is a notable increase in the CaO content, peaking at 7.49% after 1.5 hours, which suggests the decomposition of dolomite into calcite. The XRD results at this temperature level support the dolomite decomposition. The general impact of heating time in more prolonged exposure is more pronounced than the less exposure time

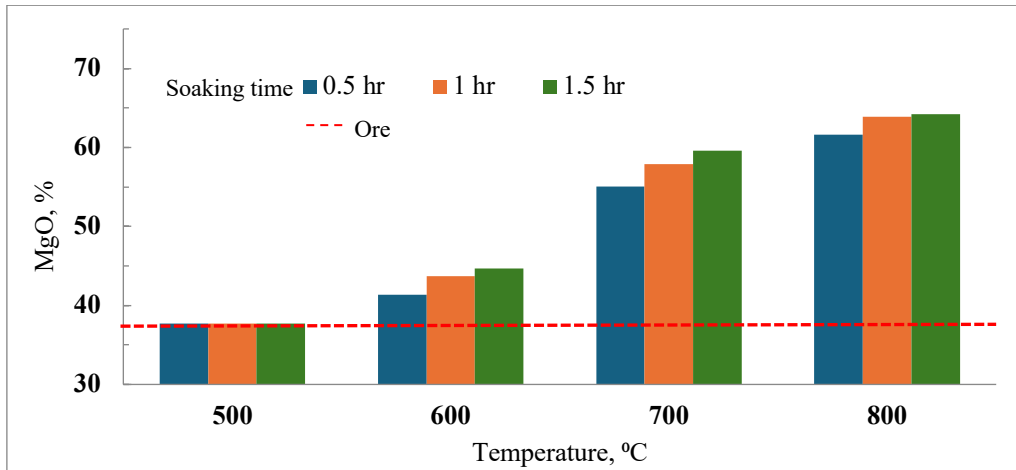


Figure 5: Influence of temperature and heating duration on MgO content.

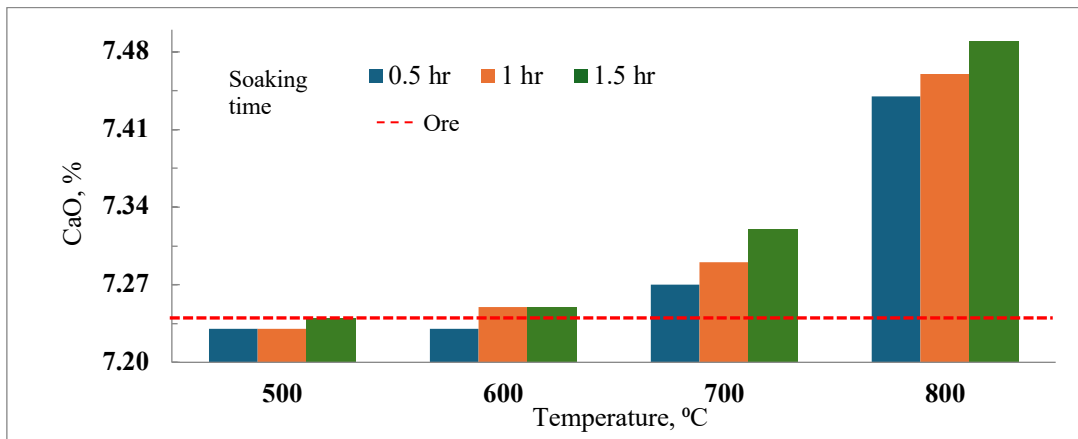


Figure 6: Influence of temperature and heating duration on CaO content.

(Figure 7) illustrates the changes in the chemical composition of Fe_2O_3 , SiO_2 , and Al_2O_3 in magnesite samples heated at temperatures ranging from 500°C to 800°C for 1.5 hours. The Fe_2O_3 content gradually increases from approximately 1.94% at 500°C to around 2.77% at 800°C , suggesting a concentration effect due to the relative stability of iron oxides. This might be indicating the phase transformation of goethite into hematite that occurred at a

temperature below 600°C [15]. However, the XRD test didn't detect the goethite face in the raw material. At the same time, the transformation of hematite to magnetite occurred at 700°C , and it is like the previous study [15,30,31]. SiO_2 and Al_2O_3 content remain stable close to the ore level in original sample at approximately 3.14% and 0.61% across all temperatures, indicating their thermal inertness.

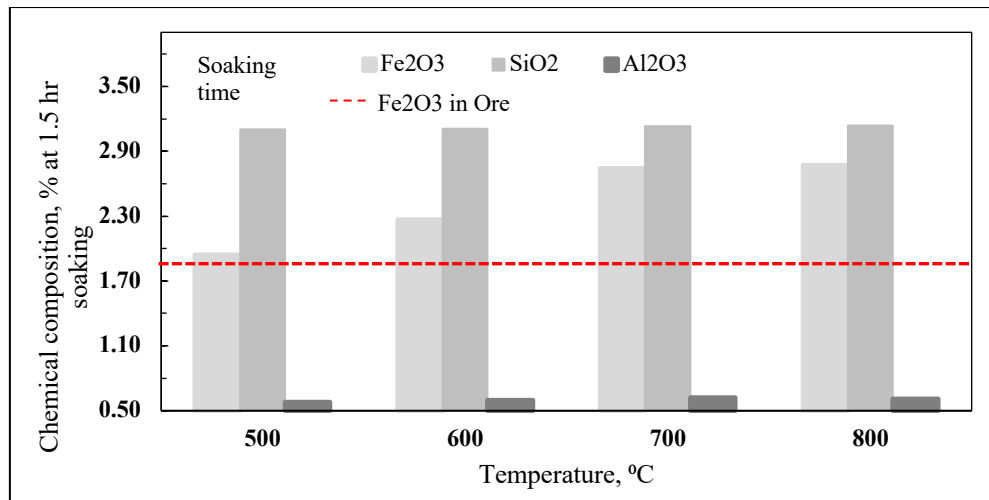


Figure 7: Influence of temperature and heating duration on CaO content.

3.3 Dry high-intensity magnetic separation

The result of Saudi low-grade magnesite ore using dry magnetic separation indicates that up to 72.32% of iron can be removed using DHIMS. This was achieved at optimal feed size ($-0.212+0.05\text{mm}$), a feed rate of 0.3 kg/min, 14 KGauss, and a roll speed of 50 rpm. Moreover, the study revealed that silica and alumina exhibit high magnetism due to the presence of clay and shale minerals, which include quartz and alumina and can bind to or physically associate with magnetic particles. The concentrate of the magnesite ore contains 40.95% MgO, 7.26% CaO, 2.14% SiO₂, 0.71% Fe₂O₃, and 0.43% Al₂O₃.

For the calcined magnesite, the chemical composition of calcined material was 59.56% MgO, 7.32% CaO, 3.13% SiO₂, 2.74 Fe₂O₃ and 0.62% Al₂O₃. After processing the material by the DHIMS, the concentrate was 67.12% MgO, 7.34% CaO, 1.74% SiO₂, 0.34 Fe₂O₃, and 0.41% Al₂O₃. In (Figure 8), the graph illustrates the reduction in the percentage of Fe₂O₃, SiO₂, and Al₂O₃ with the magnesite assay

before and after partial calcination following DHIMS application. The comparison of the reduction percentages for these impurities in magnesite samples between the two scenarios is presented. Applying DHIMS in the magnesite sample after the partial calcination process resulted in better outcomes than applying DHIMS to magnesite before partial calcination. Fe₂O₃, SiO₂, and Al₂O₃ reduction rates were significantly high in the partially calcined magnesite. Al₂O₃ decreased moderately, while SiO₂ and Fe₂O₃ showed substantial reductions. The graph demonstrates calcination's effectiveness in enhancing the magnesite's overall quality by reducing impurity levels. In the presence of magnetite, impurities such as Si and Al induce paramagnetic properties, attracting paramagnetic components to iron impurities. This phenomenon is not most likely to occur at the same rate in the case of magnesite ore samples because of the hematite. The resultant chemical composition of the concentrate of the calcined magnesite ore is 67.12% MgO, 7.34% CaO, 1.74% SiO₂, 0.34% Fe₂O₃, and 0.41% Al₂O₃.

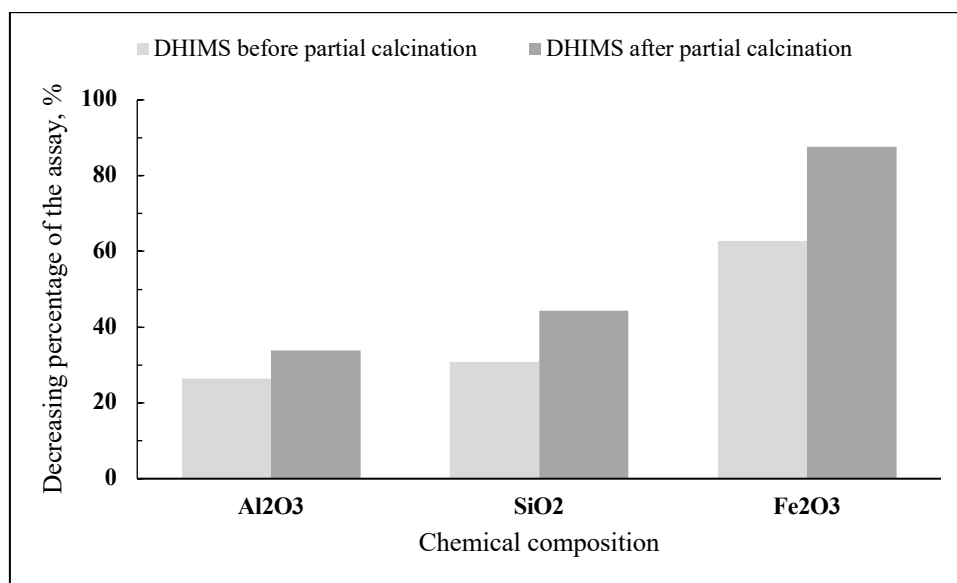


Figure 8: Decreasing the percentage of impurities in DHIMS before and after partial calcination.

4. Conclusion

The decomposition of Saudi magnesite begins at approximately 600°C, reaching its peak between 600 and 700°C. Dolomite decomposition occurs between 700 and 800°C, while the transformation of

hematite to magnetite occurs within the temperature range of 600 to 700°C. Additionally, the calcination process concentrates the magnesia, dolomite, and iron oxides. Furthermore, it enhances the removal of iron by 24.83%, silica by 13.53%, and alumina by 7.39%.

Author's Contribution:

Conceptualizations, testing and experimental work; Muhammad Hadad and Hussin Ahmed . Writing and review; Muhammad Hadad and Hussin Ahmed.

References

- [1] **Chatterjee, K.K.** Uses of Industrial Minerals, Rocks and Freshwater. vol. 53, no. 9, (2013).
- [2] **Shand, M.A.** The Chemistry and Technology of Magnesia. John Wiley & Sons, (2006).
<https://doi.org/10.1017/s1466046607070445>
- [3] **Hojamberdieva, M., Arifov, P., Tadjiev, K., and Xu, Y.** Characterization and Processing of Talc-Magnesite from the Zinelbulak Deposit. Mining Science and Technology (China), vol. 20, no. 3, pp. 415–420, (2010). [https://doi.org/10.1016/S1674-5264\(09\)60218-0](https://doi.org/10.1016/S1674-5264(09)60218-0)
- [4] **McHaffie, I.W. and Buckley, R.W.** Industrial Minerals and Rocks of Victoria; Department of Agriculture. Energy & Minerals: Victoria, Australia, (1995).
- [5] **Wang, Q.Q., Li, X.A., Wei, D.Z., and Dai, S.J.** The Application of Magnesite Processing Technics. In Applied Mechanics and Materials, Trans Tech Publ, (2011), pp. 2323–2326.
<https://doi.org/10.4028/www.scientific.net/am.m.71-78.2323>
- [6] **Chatterjee, K.K.** Uses of Industrial Minerals, Rocks and Freshwater. Nova Science Publishers, (2009).
- [7] **Shand, M.A.** The Chemistry and Technology of Magnesia. (2006).
<https://doi.org/10.1002/0471980579>

- [8] **Alvarado, E., Torres-Martinez, L.M., Fuentes, A.F., and Quintana, P.** Preparation and Characterization of MgO Powders Obtained from Different Magnesium Salts and the Mineral Dolomite. *Polyhedron*, vol. 19, no. 22–23, pp. 2345–2351, (2000). [https://doi.org/10.1016/S0277-5387\(00\)00570-2](https://doi.org/10.1016/S0277-5387(00)00570-2)
- [9] **Svoboda, J.** *Magnetic Techniques for the Treatment of Materials*. Springer Science & Business Media, (2004). <https://doi.org/10.1007/1-4020-2107-0>
- [10] **Yehia, A. and Al-Wakeel, M.I.** Talc Separation from Talc-Carbonate Ore to be Suitable for Different Industrial Applications. *Mineral Engineering*, vol. 13, no. 1, pp. 111–116, (2000). [https://doi.org/10.1016/S0892-6875\(99\)00154-5](https://doi.org/10.1016/S0892-6875(99)00154-5)
- [11] **Suvorova, D.I., Potapenko, V.E., Tyuryukhanova, V.V., Mezentsev, E.P., and Kryuchkov, V.A.** A Method of Production of Magnesite Powder of the 3-1-mm Fraction by Magnetic Separation. *Refractories*, vol. 25, no. 11–12, pp. 696–698, (1984). <https://doi.org/10.1007/bf01389943>
- [12] **Ghufon, M., Baqiya, M.A., Mashuri, M., Triwikantoro, T., and Darminto.** Phase Transition in Fe₃O₄/Fe₂O₃ Nanocomposites by Sintering Process. *Jurnal Sains Materi Indonesia*, vol. 12, no. 2, pp. 120–124, (2018). <https://doi.org/10.17146/jsmi.2011.12.2.4600>
- [13] **Wills, B.A. and Finch, J.** *Wills' Mineral Processing Technology: An Introduction to the Practical Aspects of Ore Treatment and Mineral Recovery*. Butterworth-Heinemann, (2015).
- [14] **Svoboda, J.** *Magnetic Methods for the Treatment of Minerals*. (1989). <https://doi.org/10.1155/1989/18456>
- [15] **Jang, K., Nunna, V., Sarath, H., Nguyen, A., and Bruckard, W.** Chemical and Mineral Transformation of a Low Grade Goethite Ore by Dehydroxylation, Reduction Roasting and Magnetic Separation. *Mineral Engineering*, vol. 60, pp. 14–22, Jun. (2014). doi: 10.1016/j.mineng.2014.01.021
- [16] **Genuzio, F., Sala, A., Schmidt, T., Menzel, D., and Freund, H.-J.** Interconversion of α -Fe₂O₃ and Fe₃O₄ Thin Films: Mechanisms, Morphology, and Evidence for Unexpected Substrate Participation. *The Journal of Physical Chemistry C*, vol. 118, no. 50, pp. 29068–29076, (2014). <https://doi.org/10.1021/jp504020a>
- [17] **Yuniati, M.D., Wawuru, F.C.M.P., Mursito, A.T., Setiawan, I., and Lintjewas, L.** The Characteristics of Padamarang Magnesite under Calcination and Hydrothermal Treatment. *Riset Geologi dan Pertambangan-Geology and Mining Research*, vol. 29, no. 2, pp. 153–162, (2019). <http://dx.doi.org/10.14203/risetgeotam2019.v29.1016>
- [18] **Aslani, S., Samim, R., Hashemi, B., and Arianpour, F.** Beneficiation of Iranian Magnesite Ores by Reverse Flotation Process and its Effects on Shaped and Unshaped Refractories Properties. (2009). <https://doi.org/10.1007/s12034-011-0150-0>
- [19] **Mitina, N.A., Lotov, V.A., and Sukhushina, A.V.** Influence of Heat Treatment Mode of Various Magnesia Rocks on Their Properties. *Procedia Chemistry*, vol. 15, pp. 213–218, (2015). <https://doi.org/10.1016/j.proche.2015.10.034>
- [20] **Urvantsev, A.M. and Kashcheev, I.D.** Magnesite Enrichment by a Dry Method. *Refractories and Industrial Ceramics*, vol. 53, no. 2, pp. 78–81, (2012). <https://doi.org/10.1007/s11148-012-9467-5>
- [21] **Devasahayam, S. and Strezov, V.** Thermal Decomposition of Magnesium Carbonate with Biomass and Plastic Wastes for Simultaneous Production of Hydrogen and Carbon Avoidance. *Journal of Cleaner Production*, vol. 174, pp. 1089–1095, (2018). <https://doi.org/10.1016/j.jclepro.2017.11.017>
- [22] **Mahon, D., Claudio, G., and Eames, P.** An Experimental Study of the Decomposition and Carbonation of Magnesium Carbonate for Medium Temperature Thermochemical Energy Storage. *Energies (Basel)*, vol. 14, no. 5, p. 1316, (2021). <https://doi.org/10.3390/en14051316>
- [23] **Kashcheev, I.D., Zemlyanoi, K.G., Ust'yantsev, V.M., and Voskretsova, E.A.** Study of Thermal Decomposition of Natural and Synthetic Magnesium Compounds. *Refractories and Industrial Ceramics*, vol. 56,

pp. 522–529, (2016).
<https://doi.org/10.1007/s11148-016-9880-2>

[24] **Hredzak, S., Matik, M., Lovas, M., Znamenackova, I., Stefusova, K., and Zubrik, A.** Separability of Calcined Magnesite Fines in Magnetic Field. *Inżynieria Mineralna*, vol. 16, no. 2, pp. 183–188, (2015).

[25] **Atasoy, A.** The Wet High Intensity Magnetic Separation of Magnesite Ore Waste. *Hemijska Industrija*, vol. 73, no. 5, pp. 337–346, (2019).
<https://doi.org/10.2298/HEMIND181010026A>

[26] **Yehia, A. and Al-Wakeel, M.** Role of Ore Mineralogy in Selecting Beneficiation Route for Magnesite-Dolomite Separation. *Physicochemical Problems of Mineral Processing*, vol. 49, (2013).

[27] **Bentli, I., Erdogan, N., Elmas, N., and Kaya, M.** Magnesite Concentration Technology and Caustic–Calcined Product from Turkish Magnesite Middlings by Calcination and Magnetic Separation. *Separation Science and Technology*, vol. 52, no. 6, pp. 1129–1142, (2017).
<https://doi.org/10.1080/01496395.2017.1281307>

[28] **Ignjatović, M.R., Čalić, N., Marković, Z.S., and Ignjatović, R.** Development of a Combined Gravity–Magnetic Separation Process for Magnesite Ore Using HGMS. *Physical Separation in Science and Engineering*, vol. 6, pp. 161–170, (1995). <https://doi.org/10.1155/1995/71218>

[29] **Olszak-Humienik, M. and Jablonski, M.** Thermal Behavior of Natural Dolomite. *Journal of Thermal Analysis and Calorimetry*, vol. 119, pp. 2239–2248, (2015).
<https://doi.org/10.1007/s10973-014-4301-6>

[30] **Gaviria, J.P., Bohé, A., Pasquevich, A., and Pasquevich, D.M.** Hematite to Magnetite Reduction Monitored by Mössbauer Spectroscopy and X-Ray Diffraction. *Physica B: Condensed Matter*, vol. 389, no. 1, pp. 198–201, (2007).
<https://doi.org/10.1016/j.physb.2006.07.056>

[31] **Witte, K., Bodnar, W., Schell, N., Fulda, G., and Burkel, E.** Phase Transformations of Stoichiometric Mixtures of Hematite and Iron under FAST Conditions. *Journal of Alloys and Compounds*, vol. 724, pp. 728–734, (2017).
<https://doi.org/10.1016/j.jallcom.2017.07.089>

نأثير المعالجة الحرارية على إزالة الشوائب من الماجنيزيت باستخدام الفصل المغناطيسي الجاف عالي المجال

محمد. الحداد وحسين أحمد

جامعة الملك عبد العزيز، جدة، كلية الهندسة، قسم هندسة التعدين

malawialhaddad@stu.kau.edu.sa

المخلص: تتناول هذه الدراسة التخلص من الشوائب المصاحبة لخام الماجنيزيت السعودي ذو الدرجة المنخفضة الذي يتكون من: 37.68% MgO، 7.24% CaO، 3.10% SiO₂، 1.91% Fe₂O₃، 0.58% Al₂O₃، و48.65% LOI. ودراسة عملية التحميص وإزالة الشوائب الناتجة. حيث تم استخدام الفصل المغناطيسي الجاف عالي الكثافة التخلص من الشوائب المصاحبة لخام الماجنيزيت السعودي ذو الدرجة المنخفضة قبل وبعد عملية التحميص. تم دراسة عدة عوامل، بما في ذلك حجم الماجنيزيت، ومعدل التغذية لجهاز الفصل، وقوة المجال المغناطيسي، وسرعة الأسطوانة، باستخدام فاصل مغناطيسي أسطواني من أوتوك (طرارز). (5-111-13 MIH تظهر النتائج أن إزالة الشوائب أكثر كفاءة بعد عملية التحميص مقارنةً بما قبلها. ومن المتوقع أن يكون المنتج النهائي مادة خام مناسبة لإنتاج الماغنيسيا المحروقة، والتي تُستخدم في صناعة المواد المقاومة للحرارة